TRANSPORT PROBLEMS 2022 Volume 17 Issue 4
PROBLEMY TRANSPORTU DOI: 10.20858/tp.2022.17.4.08

Keywords: civil engineering; transport; mobile platforms; welding; 316L steel

Bożena SZCZUCKA-LASOTA[1], Tomasz WĘGRZYN[2]*

IMPROVEMENT OF THE MECHANICAL PROPERTIES OF MOBILE PLATFORM STAINLESS CONSTRUCTION ELEMENTS

Summary. Stainless steel could be treated as the main material used to construct various means of transport, including mobile platforms and tank trucks. An austenitic steel known as 316L steel (1.4401) has high resistance to atmospheric corrosion, natural waters, water vapor, alkaline solutions, and acids, even at elevated temperatures. This steel is weldable, although it is also prone to various types of welding cracks. Many factors influence the quality and mechanical properties of a joint. The most significant of these is the appropriate selection of welding parameters, which should be determined precisely and separately for each type of sheet, depending on its thickness and geometric features. The aim of the present article is to study the influence of main TIG (Tungsten inert gas) welding parameters on the creation of proper joints used in the construction of mobile truck platforms or tank trucks. The proper selection of parameters enables the production of welds with good functional properties. A novelty of this article is the proposal to weld each layer of a thick joint with different parameters, which has an important influence on the mechanical properties of the joint. It is expected that the new material and technological solution will yield a joint with good corrosion resistance and increased mechanical properties. This is important in the responsible construction of means of transport, using the example of mobile platforms and tank trucks. Different tests verifying the properties of joints, including non-destructive testing, tensile strength tests, and fatigue tests, as well as a hardness probe, were applied.

1. INTRODUCTION AND TRANSPORT RESEARCH PROBLEM

In the structural elements of mobile platforms, non-alloy, high-strength, stainless austenitic and austenitic-ferritic steels are applied. The specific means of transport in which corrosion is a challenge in terms of materials and technology are a mobile platform and tank truck. The elements of the mobile landing are often subjected to corrosion, which threatens the safety of the structure and workers. One defense against this problem is the use of stainless steel for structural components exposed to corrosion; thus, various types of structural steel, both unalloyed and alloyed, play an important role in the automotive industry [1]. Certain structural elements of a platform should have a high ultimate tensile strength (UTS) and acceptable plastic properties, particularly yield stress to ensure the lowest possible weight of such transport means. Meanwhile, other elements exposed to frequent contact with water and mud should be corrosion-resistant and have a high short-term strength limit of at least 500 MPa [2]. The elements of some means of transport are in frequent or permanent contact with moisture, water, and seawater and, thus, are prone to corrosion. The problem of corrosion in some means of transport can lead to numerous hazards. An example of such a hazard in transport is the corrosion of

[1] Silesian University of Technology; 8 Krasińskiego, 40-019 Katowice, Poland; e-mail: bozena.szczucka-lasota@polsl.pl; orcid.org/0000-0003-3312-1864
[2] Silesian University of Technology; 8 Krasińskiego, 40-019 Katowice, Poland; e-mail: tomasz.wegrzyn@polsl.pl; orcid.org/0000-0003-2296-1032
* Corresponding author. E-mail: tomasz.wegrzyn@polsl.pl

steel elements in mobile platforms and tank trucks. Corroded elements reduce the load capacity or anchoring of the structure, which reduces the safety of the work performed, especially at high altitudes. Fig. 1 shows an example of highly loaded elements in a mobile platform that should have higher corrosion resistance.

Fig. 1. Visible corrosion in the central part of the mobile platform (specific means of transport)

Fig. 2 is a detailed view of the corrosion effect of the platform structure element after a long period of operation. Such corroded elements lose their required mechanical properties.

Fig. 2. Element of the mobile platform with various levels of corrosion intensity

Attempts are being made to use more stainless steel in order to avoid frequent repairs to vehicle components exposed to corrosion. In particular, austenitic steels have been extensively used in the structure of different types of means of transport, including the construction of mobile platforms.

Austenitic steels also show excellent plastic properties, as indicated by their impact strength above 50 J, even up to -200 °C. Compared to structural steels, austenitic stainless steels have higher thermal expansion and a shrinkage of approximately 40%, which creates various welding problems [3]. In the automotive industry stainless steel is used for connecting rods, crankshaft components, gears, bearing caps, turbocharger components, exhaust system components, interior mirror mounts, seat belt latches, window lifter components, and more. Selected applications of stainless steels in the automotive industry are listed below with examples of steel grades [4]:

- exhaust system,
- housings of catalysts and turbochargers,
- internal components of catalysts,
- internal components of turbochargers (rotors),
- safety cages (Fig. 1),

- vehicle tanks,
- fuel tanks,
- clamps,
- chassis.

316 L steel is applied for various thin-walled construction (thickness = 2 mm) in automotive transport. An example of an austenitic element in an automotive structure is shown in Fig. 3.

Fig. 3. A motor vehicle end muffler tip made of stainless steel

Thicker stainless steel structures (above 5 mm) tend to crack if the welding parameters are not correct. The incorrect selection of linear energy when welding 316L steel (above 1.2 kJ/mm) can contribute to the molding of different non-metallic inclusions, especially carbides of the $M_{23}C_6$ type, as well as intermetallic inclusions, especially of the sigma phase (FeCr), leading to the phenomenon of intercrystalline or stress corrosion, which causes a decrease of strength and a reduction in the ductility of the material. Additional filler materials must be applied with a carbon content reduced several times to approximately 0.02% to prevent the described negative phenomena when welding 316L steel (containing 0.07% C) in the tungsten inert gas (TIG) process [7-8]. Lowering the carbon content in an austenitic weld is beneficial, as it might promote the precipitation of delta ferrite. It might also reduce the content of $M_{23}C_6$ carbides at the austenite grain boundaries for two reasons [9]. First, the amount of carbides in steel/weld metal depends on the carbon percentage in the steel/weld metal; similarly, the number of non-metallic oxide/nitride inclusions in the steel/weld metal deposit depends on the O and N content of both the steel and filler material. Second, an analysis of the temperature-time-transformation graph shows that, during joint cooling under welding conditions in a weld metal containing 0.07% C, carbides begin to form at the temperature of 800 °C after one minute. In a weld metal containing 0.02% C, carbides begin to form at 550 °C after 100 hours.

The presence of $M_{23}C_6$ carbides in an austenitic weld is disadvantageous, as it causes intercrystalline corrosion. The main component of carbides is chromium (80%). When carbides are formed, the border parts become deficient in chromium, making the joint prone to corrosion in these areas [4,7]. Cracks in austenitic steel joints may occur when too much heat is applied during welding. The selected welding process should ensure that the important welding parameter, time $t_{8/5}$ (time 800–500), is appropriate. That is, the time it takes for the material to cool from 800 °C to 500 °C after welding should be short, as this temperature range promotes unfavorable non-metallic inclusions, thus deteriorating the plastic properties of the joint. One-phase austenitic steel has a strong tendency to crack soon after welding. Apart from austenite, stainless steels should contain a small amount of delta ferrite (3–8%) to reduce the tendency to hot cracking, as delta ferrite dissolves impurities (O, S, P) better than austenite. The presence of ferrite in a joint may limit the content of unfavorable sulfide, oxide, and phosphorus inclusions, which affect weld ductility [7-8]. Although phosphorus dissolves well in steel (in austenite up to 0.5% P, in ferrite up to 2.5%), during the cooling process of steel under welding conditions, phosphides Fe_2P and Fe_3P may form, causing cold cracks (cold brittleness). On

the other hand, the presence of sulfur in steel promotes hot brittleness [10-12]. In austenitic steels, hardening and hydrogen cracks do not appear, as the solubility of hydrogen in austenite is four times greater than in alpha ferrite [11]. Therefore, preheating these steels prior to welding is not necessary as long as the ambient temperature is above 5 °C. Due to the possibility of cracking, an interpass temperature must be severely limited to approximately 100 °C for austenitic steels and up to 150° C for austenitic steel with delta ferrite [11]. Welded joints used for the austenitic steel components of means of transport must be characterized by good corrosion resistance, high UTS, adequate ductility, and a good fatigue limit. The fatigue process data play an important role in the assessment of the weldability of austenitic steels used in the construction of means of transport due to the safety of the structure.

Research on mobile platforms shows that cracks in joints (Fig. 4) are one of the main causes of serious failures of these structures. Previous articles [14-16] present examples of damage to mobile platforms as a result of improperly performed welds.

Fig. 4. Cracks in a weld

Therefore, it is vital to use an appropriate material and technological process. The aim of the present article is to study the influence of main TIG welding parameters on the formation of correct thicker welds used in the construction of mobile platforms or tank trucks. The tests involved checking the following welding current and voltage parameters:

- the lower stitch pattern, including the type of current and polarity,
- the upper stitch pattern, including the type of current and polarity,
- welding speed.

The manufactured welded joints (described in section 2) were subjected to non-destructive and destructive tests (described in section 3).

2. MATERIALS

An austenitic sheet (316L) was chosen to create the elements of a mobile platform. The selected process parameters included influencing weld geometry (shape), the proper bevelling method, as well as a thorough analysis of the most important welding parameters, such as welding current and speed, which have a direct impact on the $t_{8/5}$ time (the time it takes for the weld seam and adjacent heat-affected zone (HAZ) to cool from 800 °C to 500 °C). The materials used for the tests were welded joints made from austenitic 316L steel using the TIG (141) method. Gas tungsten arc welding (GTAW), also known as welding with the TIG, yields high-quality welded joints. The 141 method is based on the use of a non-consumable W (tungsten) electrode in a shield of inert gases such as argon, helium, or their combination. Among all types of GTAW welding, the 141 method has the widest range of possibilities. The main feature of this method is the argon stream exiting the torch nozzle,

which effectively protects the welding area from contact with air, eliminating the processes of oxidation and nitriding. If necessary, the filler wire is also manually fed into the arch [17-18]. Information about the main 316L steel marks is presented in Table 1.

Table 1

316L steel used in tests using the nomenclature according to various standards

Other symbols/standards			
PN	ASTM	AISI	EN
00H17N14M2	1.4404	316L	X2CrNiMo17-12-2

The main properties of the acid-resistant 316L steel and the weld metal deposit of the two tested wires are presented in Table 2.

The composition of 316L steel and the weld metal of tested electrode wires with various amounts of carbon are presented in Table 3.

Table 2

Properties of steel

Steel	Yield stress (YS), MPa	Ultimate tensile strength (UTS), MPa	Brinell hardness, MPa
316L	240	610	200

Table 3

Composition of the steel 316L and weld metals of the wires

Composition of	C, %	Mn, %	Si, %	Mo, %	Ni, %	Cr, %	P, %	S, %
316 L	0.07	2.1	1.05	2.5	13.1	18.6	0.044	0.015
Filler material Lincoln LNT 316L	0.02	1.4	0.85	2.6	12.6	19.1	0.021	0.021

Table 3 shows that, apart from the C content, the chemical compositions of the welded steel and the filler material are very similar.

3. RESEARCH METHODS

The joints were made from 316L steel with a thickness of 6 mm in a flat position with standard V beveling. The shape and the method of placing subsequent layers are presented in Figs. 5 and 6.

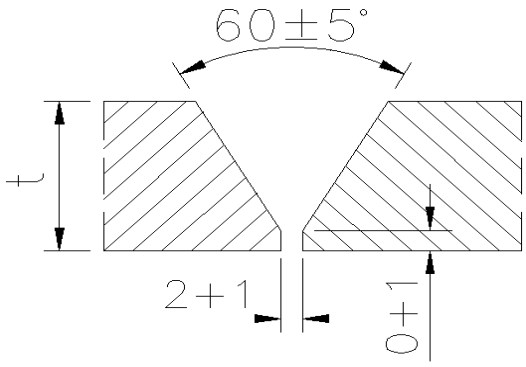

Fig. 5. Details of the chamfering

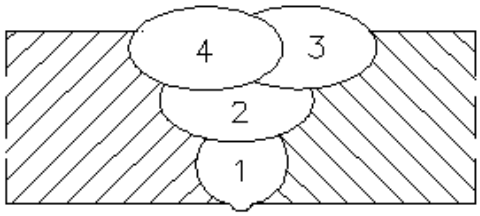

Fig. 6. The method of arranging subsequent layers with the use of the TIG process

After welding, the samples for non-destructive tests (NDTs) were prepared. Visual tests (VTs) were carried out in accordance with the PN-EN 970/1999 norm. This research allowed for assessments of the joints, identification of any incompliances (mainly cracks), and the elimination of incorrectly prepared welds. The tests were extended to include penetrant (PN-EN-571/1999) and ultrasonic (PN-EN:1714/2002) methods. The welded joints were also studied with the use of destructive tests. A bending test was performed in accordance with the EN ISO-5173-201 standard. The tensile test was realized according to the PN-EN-ISO-6892-1/2020 standard. A hardness test was done according to the PN-EN ISO 9015-1/2011 standard.

First, the following parameters were checked:
- welding current (I_1) for the first layer,
- arc voltage (U_1) for the first layer,
- welding speed (v_1) for the first layer,
- welding current (I_n) for the next layer,
- arc voltage (U_n) for the next layer,
- welding speed (v_n) for the first layer,
- type of current (direct or alternating),
- polarity (-, ~),
- type of shielding gas and its flow rate.

The analyzed paper [13] presented fractographic evidence of the cracking of austenitic steels used for tanks. These cracks were the result of excessive residual restraint stresses. As demonstrated by the authors of the study, the cracks occurred as a result of seam matching and the welding practice used, as the same welding parameters for each sequence of welds were used at the final closure of the tank. This article does not provide a solution to this problem. Therefore, the authors decided to select and control the parameters separately for all welded layers. Based on the analysis of the literature, it was found that the proposed modification of the process should have a positive influence on an obtained structure and the properties of the welded joint, as a properly made weld will ensure the safety of a mobile elevating work platform [14].

When giving the lower (first) layer, the current I_1 was modified in the range of 70–100 A. Arc voltage U_1 was changed in the range of 9–11 V. Welding speed v_1 was modified in the range of 60–120 mm/min. The welds were formed using alternating current or direct current (with only negative polarity on the electrode). The only shielding gas in TIG was argon. The Ar flow rate was fixed at the level of 12 l/min in all tested cases. Due to the shape of the first stitch (root layer) and in order to obtain the highest-quality joint possible, the following welding parameters were selected:

- $U_1 = 10$ V,
- $I_1 = 70$ A,
- $v_1 = 60$ mm/min.

In the next stitches of the weld, the current I_n was increased to either 100 A or 130 A. The arc voltage U_n was generally on the level of 10 V and was slightly modified up to 13 V both during direct current (DC) and alternating current (AC) welding. The welding velocity v_n was changed in the range of 60–120 mm/min. The effect of varying the type of welding current (AC or DC) by installing a negative polarity at the electrode was also investigated. It was agreed that the interpass temperature would not exceed 150 °C. There were concerns that due to the differences in the carbon content in the steel and in the filler material, uncontrolled precipitation of delta ferrite content in the weld may occur (Table 3). The test results are presented in the next section (Table 5). The next stage of the research

was the bend test, for which only those joints that showed no defects and incompatibilities for level B (samples S4, S5, S7) were selected.

The bending test was performed based on the EN-ISO-5173-2010 standard. For the bending tests, 10 samples with a thickness of 6 mm and a width of 10 mm were prepared. The mandrel diameter was 32 mm, and the roll distance was 54 mm. The bending angle was 180°. Five measurements of joint bending from the side of the weld face and five measurements of the weld from the side of the root were made.

The next part of the research included joint tensile tests. The measurements were carried out on a ZWICK 100N5A machine.

The microstructure of welded joints was tested by light microscopy (Olympus Microscopy).

4. RESULTS AND ANALYSIS

The results obtained from the NDT tests are presented in Table 4. This table summarizes our observations (Fig. 7) for this first round of tests.

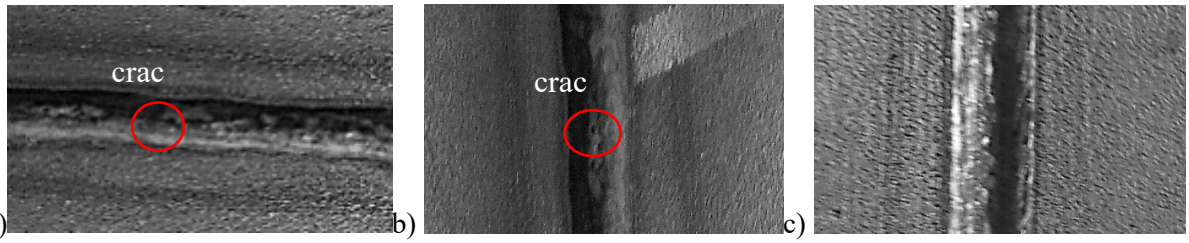

Fig. 7. The image of some specimens (a-b) with cracks or (c) a lack of cracks

An analysis of the test NDT results shows that incorrectly chosen welding parameters led to the formation of cracks in the weld joint.

The most important observation is the correct choice of a power source. In the case of alternating current, cracks always occurred (samples: S1, S2, S6, S9). Cracks were observed because less heat was supplied to the weld pool in the welding process with negative polarity at the electrode than when an alternating current is used. This affects the metallurgical and thermodynamic processes of the solidification and cooling of the weld. Another important parameter is the welding speed. For the sheet thickness considered, the most appropriate speeds are 80 mm/min and 100 mm/min.

If the welding current or arc voltage is too high, cracks will form. The welding speed of 120 mm/min is clearly incorrect (samples S8, S9, S10). Current intensity and welding speed affect the linear energy of the process, which determines the quality of the joint.

By slightly changing the welding parameters in 10 cases (samples S1–S10), only few positive test results were obtained (samples S4, S5, S7).

Based on the non-destructive tests (Table 4), some main conclusions can be presented:

- Short cracks in the range of 1.5 to 5 mm occurred in the case of poorly selected welding parameters.
- It is recommended to use a direct current with negative polarity on the electrode instead of an alternating current.
- A lack of welding defects and incompatibilities for the B level (with PN-EN ISO-5817: 2005) were observed for joints obtained with lower linear energy (S7, S5, S4).

Only the joints that presented a lack of defects and incompatibilities for level B were chosen for further testing (bending). For the joints of S7, S5, and S4, the bending test was realized in accordance with the EN-ISO-5173-2010 norm. After the bending test, visual tests (VTs) were carried out with an eye and magnifier (at triple magnification). These visual tests (VTs) were carried out following the PN-EN-ISO-17638 standard. In all tested cases, during visual tests (VTs), no cracks were found in the weld or HAZ at a bending angle of 180°. The bending test results clearly show that the welded joints (S4, S5, S7) were appropriate and that the welding parameters were correctly chosen.

Table 4

NDT results and observations

Specimen mark	Parameters of the first stitch U_1 [V], I_1 [A], v_1 [mm/min] / current	Parameters of the first stitch U_n [V], I_n [A], v_n [mm/min] / current	NDT results, observation
S1	10 V, 70 A, 60 mm/min, „~”	10 V, 100 A, 60 mm/min, „~”	cracks in the joint
S2	10 V, 70 A, 60 mm/min, „-„	10 V, 100 A, 60 mm/min, „~”	cracks in the joint
S3	12 V, 70 A, 60 mm/min, „-„	13 V, 115 A, 60 mm/min, „-„	cracks in the joint
S4	10 V, 70 A, 60 mm/min, „-„	10 V, 115 A, 80 mm/min, „-„	no cracks
S5	10 V, 70 A, 60 mm/min, „-”	10 V, 130 A, 80 mm/min, „-„	no cracks
S6	10 V, 70 A, 60 mm/min, „-„	13 V, 100 A, 100 mm/min, „~”	cracks in the joint
S7	10 V, 70 A, 60 mm/min, „-„	10 V, 115 A, 100 mm/min, „-„	no cracks
S8	10 V, 70 A, 60 mm/min, „-„	10 V, 130 A, 120 mm/min, „-„	cracks in the joint
S9	10 V, 70 A, 60 mm/min, „~”	10 V, 100 A, 120 mm/min, „~”	cracks in the joint
S10	10 V, 70 A, 60 mm/min, „-„	13 V, 100 A, 120 mm/min, „-„	cracks in the joint

In the next point of the investigation, the same samples (S4, S5, S7) were tested on a ZWICK 100N5A machine. The tensile strength results for the joints are presented in Table 5.

The results of the tensile tests were positive. All joints were characterized by a high value of ultimate tensile strength above 500 MPa, which is the recommended value for the structure of stainless steel for automotive needs.

Table 5

Tensile strength of the tested joints

Specimen	UTS, MPa	σ (UTS), MPa	Elongation, %	σ (Elongation), %
S4	535	1.65	27	0.78
S5	517	1.82	26	0.86
S7	521	1.77	25.5	0,75

There were no substantial differences between the mechanical test results for the samples. For S4, we registered elongation at the level of 27% and tensile strength of 535 MPa. In the next step, only the microstructure of the S4 joint was characterized (Fig. 7).

The dominant structure of the steel and weld was austenite. A two-phase structure was visible on the fusion line. Delta ferrite precipitates are obtainable between the austenitic forms of the dendrites. This is a result of the 2.5-times smaller C content introduced into the joint from the filler material. Carbon is a strong austenite-forming factor; therefore, lowering its content in the material such that the structure based on the chemical composition (see the blue area on the Schaeffler diagram in Fig. 7) towards the boundary area of austenite and delta ferrite (indicated by the red arrow and green area in Fig. 7).

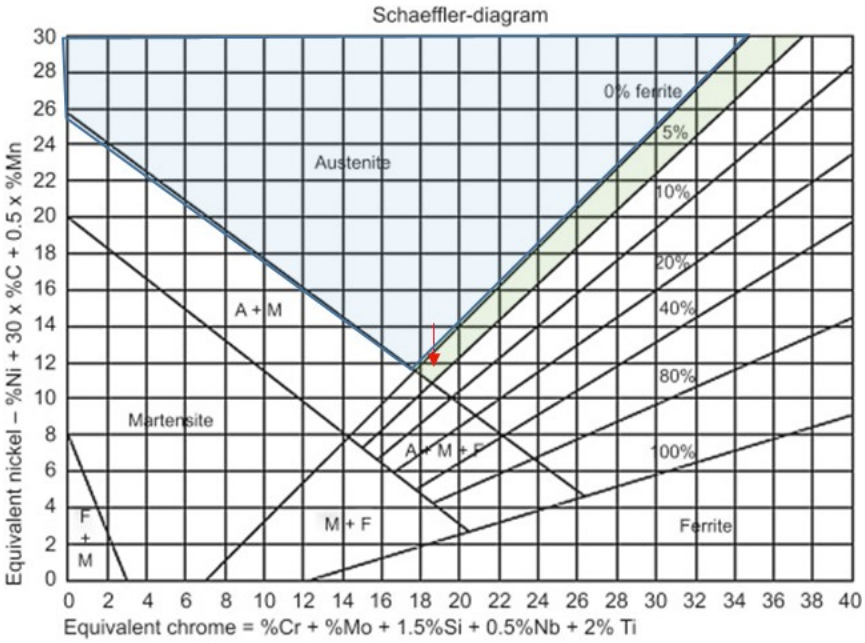

Fig. 8. Schaeffler diagram with marked areas of austenite (blue area) and austenite with low ferrite content (green area)

To maintain a 100% austenitic structure, a filler material with increased carbon content might be proposed, because C is austenite former element (Fig. 8). However, it is be recommended, as increased carbon content in the weld results in the formation of carbides, which is less advantageous than the presence of a low delta ferrite content. As a result of correctly chosen welding parameters, ferrite delta is fine-grained. An increase in the welding of linear energy promotes the growth of ferrite grains, which leads to the formation of cracks (as observed in S1, S2, S3, S6, S8, S9, S10; Table 3). The last stage of the experimental approach was to measure the hardness HV in the central part of the weld. The tests were realized as usual for S4, S5, and S7 because these specimens did not have any welding defects. Very often, the tensile strength tests described in the literature, in combination with non-destructive tests, are the main criterion for qualifying materials and technologies for use in the construction of means of transport.

By definition, a suitably made austenitic steel joint has good plastic and mechanical properties (40% and 500 MPa, respectively) [15-16]. In the analyzed case, this approach is insufficient because the estimated value of the fatigue limit reached 165 MPa. Meanwhile, in the case of welded structures intended for tank truck construction, stainless steel additionally requires good fatigue resistance. This means that the joint at the mentioned value of the mechanical property can be approved for use. Therefore, the test under one-axial cyclic loading was performed using the fatigue limit value of 200 MPa. In this case, flat specimens (as a confidential project of a third party) were used. They were subjected to cyclic loading represented by a cyclic displacement signal in the form of a sinusoidal function with a frequency of 10 Hz and R=-1. As a practical aspect, the loading stage was designed to determine the stress at which no failure would occur after 2×106 cycles. This was directly connected to the experimental procedure proposed by a company, and it was restricted by the time with respect to the inspection process and a lowering of cost due to downtime. The values of the fatigue limit is presented in Table 6. That is, the limit values of the range differed by only 45 MPa, and therefore, the values that followed this range can be averaged. As a result, the obtained value of the fatigue limit was 203 MPa.

The results presented in Table 6 show that the fatigue strength of all tested joints varied considerably.

Nevertheless, considering the noteworthy details shown in Table 6, the best results were obtained for S4 (similar to the previous cases). Thus, it is possible to indicate the best welding parameters. It

can be concluded that only the following welding parameters are suitable for the execution of the best four-pass joint of austenitic steel sheets with a thickness of 6 mm:
- lower stitch pattern (No. 1 in Fig. 6): voltage U_1 = 10 V, amperage I_1 = 70 A, and speed v_1 = 60 m, direct current with negative polarity at the electrode;
- upper stitch pattern (No. 2–4 in Fig. 6): voltage U_n = 10 V, amperage I_n=115 A, speed of the process: v_1 = 80 mm/min.

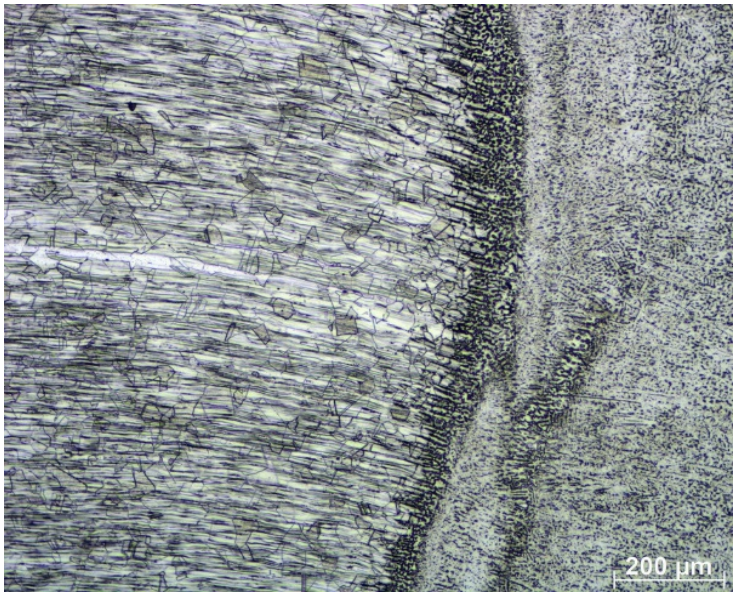

Fig. 9. The microstructure of the S4 joint made of 316 L steel etched with 10% oxalic acid

Table 6

Fatigue limit of the tested joints

Specimen	Base material, MPa	Welded joint, MPa
S4	265	230
S5		185
S7		195

5. DISCUSSION

The results presented in the previous chapter indicate that the two-phase structure connections made with low linear energy (below 1.2 kJ/mm) were of good quality and were not susceptible to hot cracks. The connections were characterized by good mechanical properties, UTS, and relative elongation. So, we expect an increase in interest in austenitic steels for the construction of safe structures in the automotive industry. Until now, in the welding of austenitic steels, it was believed that the most important task was to obtain a joint with good corrosion resistance without cracks and other welding defects. However, this article shows that the choice of welding parameters for each layer in the thicker joint has an impact on the mechanical properties. It has a profound impact on the proper exploitation of means of transport in mobile platforms, tank trucks, and dump trucks (Fig. 10).

Indicating how much the careful selection of welding of each layer of the joint influences the different properties of a weld (especially its fatigue strength) is a novelty in terms of materials and technology of austenitic steel structures for automotive applications.

6. CONCLUSIONS

This study analyzed the possibility of producing the stainless elements of means of transport using the example of mobile platform supports. High corrosion resistance is also required in other means of

transport, especially tank trucks. In the present work, the welding of austenitic elements (316L steel) was carefully tested. Welding austenitic steel is very difficult. For each thickness of a joint of variable mass and shape, precise tests should be performed separately, taking into account all welding parameters. In addition to good anti-corrosion properties, joints in means of transport must have good mechanical properties in order to ensure the safety of the structure. Some elements are prone to hot welding cracks with poorly selected welding parameters. It is very difficult to select the best welding parameters for austenitic steel. It is important to determine the shape of the edge of the plates before welding (bevelling method). It is also important to select appropriate electrode wires, shielding gases, current-voltage parameters, and welding speeds.

Fig. 10. A vehicle with highly loaded elements of a tipper made of austenitic steel

Ten test joints were created for this research using different welding parameters to demonstrate the influence of the proper selection of welding parameters with low linear energy on the quality, structure and properties of joints. After the welds were made, non-destructive tests (NDTs) were performed. It was discovered that only three connections (S4, S5, S7) with low linear energy below 1.2 kJ/mm were of good quality. During further destructive tests, only joints without welding incompatibilities (S4, S5, S7) were further verified. Bending tests revealed that none of the mentioned joints had any cracks. Similarly, the tensile strength results showed the satisfactory properties of the joints (good UTS and elongation). The structure studies confirmed that ferrite delta forms could be present in the weld. The bi-phase composition of the weld (approximately 97% austenite, 3% ferrite) could be considered a much more favorable structure than the single-phase austenite, which is prone to welding cracks. It was also shown that precisely indicated welding parameters were selected correctly, as very good properties of the joint were obtained. Based on the results, the following main conclusions were drawn:

- The best results when creating austenitic structures of means of transport were obtained when TIG welding was realized with a direct current (DC) with negative electrode polarity.
- The linear welding energy should not exceed 1.2 kJ/mm.
- Using a material filler with a lower carbon content than 316L steel may lead to delta ferrite formation.
- The interpass temperature may not exceed 150 °C due to the two-phase structure of the weld.
- TIG welding can be used in construction in the automotive industry, as it yields high-quality joints.

Acknowledgment

This paper is a part of the COST project, CA 18223. Part of the presented research was funded by the Silesian University of Technology grant BK-270-RT

Reference

1. Niedzielska, M. & Chmielewski, T. HVOF spraying process conditions of coating Cr_3C_2-NiCr deposited onto 316L steel. *Welding Technology Review*. 2017. Vol. 89. No. 3. P. 46-50.
2. Frazier, W.E. & Polakovics, D. & Koegel W. Qualifying of Metallic Materials and Structures for Aerospace Applications. *JOM*. 2001. Vol. 53. P. 16-18.
3. *Stal nierdzewna w przemyśle samochodowym*. Available at: http://www.stalenierdzewne.pl/662/stal-nierdzewna-w-przemysle-samochodowym. [In Polish: Stainless steel in the automotive industry]
4. Folkhard, E. Welding Metallurgy of Austenitic Stainless Steels. In: *Welding Metallurgy of Stainless Steels*. Springer. Vienna. 1988. DOI: https://doi.org/10.1007/978-3-7091-8965-8_9.
5. Euro-Inox. *Guidelines of the Welded fabrication of Stainless steels*. 2007.
6. Sowards, J. & Caron, J. Weldability of Nickel-Base Alloys. In: Saleem Hashmi (ed.) *Comprehensive Materials Processing*. Elsevier. 2014. Vol. 6. P. 151-179.
7. Herderick, E. Additive manufacturing of metals. A review. In *Mater Sci Technol Conf. exhib. 34 2011, MS&T'11*. 2011. Vol. 2. P. 1413-1425.
8. Benson, T.H. & Shoeppner, G.A. Accelerating Materials Insertion by Evolving DoD Materials Qualification-Transition Paradigm. *AMMITAC Q*. 2002.Vol. 6. No. 1. P. 3-6.
9. Tarasiuk, W. & Golak, K. & Tsybrii, Y. &, Nosko, O. Correlations between the wear of car brake friction materials and airborne wear particle emissions. *Wear*. 2020. Vols. 456-457. Paper No. 203361.
10. Pałubicki, S. & Karpiński, S. Linear energy impact on formation of hot cracks in the welding process of S 355J2WP by 135 method. *Welding Technology Review*. 2015. Vol. 87. No. 4. P. 21-27.
11. Ramon, J. & Basu, R. & Voort, G.V. & Bola, G. A comprehensive study on solidification (hot) cracking in austenitic stainless steel welds from a microstructural approach. *International Journal of Pressure Vessels and Piping.* 2021. Vol. 194. Part B. No. 104560.
12. Celin, R. & Burja, J. Effect of cooling rates on the weld heat affected zone coarse grain microstructure. *Metallurgical and Materials Engineering*. 2018. Vol. 24. No. 1. P. 37-44.
13. James, M.N. & Matthews, L. & Hattingh, D.G. Weld solidification cracking in a 304L stainless steel water tank. *Engineering Failure Analysis.* 2020. Vol. 115. Paper No. 104614.
14. Martinetti, A. & Chatzimichailidou, M.M. & Maida, L. & van Dongen, L. Safety I–II, resilience and antifragility engineering: a debate explained through an accident occurring on a mobile elevating work platform. *International journal of occupational safety and ergonomics*. 2019. Vol. 25. No. 1. P. 66-75.
15. Gao, X. & Sun, D. & Ge, Y. & Yang, X. & Li, J. Dynamic stability analysis and experiment of the mobile elevating work platforms. In: *IOP Conference Series: Materials Science and Engineering.* 2020. Vol. 772. No. 1. Paper No. 012013.
16. Bošnjak, S.M. & Gnjatović, B.N. & Momčilović, D.B. &. Milenović, I.L.J. & Gašić V.M Failure analysis of the mobile elevating work platform. Case Studies in Engineering. *Failure Analysis.* 2015. Vol. 3. P. 80-87.
17. Urzynicok, M. & Kwieciński, K. & Szubryf, M. & Slania, J. Application of new GMAW welding methods used in prefabrication of P92. P. 532-541. Available on: https://www.osti.gov/etdeweb/biblio/21588204.
18. Rogalski, G. & Świerczyńska, A. & Landowski, M. & Fydrych, D. Mechanical and microstructural characterization of TIG welded dissimilar joints between 304L austenitic stainless steel and Incoloy 800HT nickel alloy. *Metals*. 2020. Vol. 10. No. 5. P. 559-570.

Received 15.06.2021; accepted in revised form 23.11.2022